


Article

Investigation on the Through-Thickness Temperature Gradient and Thermal Stress of Concrete Box Girders

Qiangru Shen ^{1,2}, Jingcheng Chen ¹, Changqi Yue ³, Hui Cao ¹, Chong Chen ⁴ and Wangping Qian ^{1,*} 

¹ School of Transportation and Civil Engineering, Nantong University, Nantong 226019, China; shenqr@ntu.edu.cn (Q.S.)

² Department of BIM Research, Nantong Institute of Technology, Nantong 226001, China

³ School of Civil Engineering and Transportation, South China University of Technology, Guangzhou 510641, China

⁴ Nantong Transportation Bureau, Nantong 226018, China

* Correspondence: qianwangping@my.swjtu.edu.cn

Abstract: Bridges are generally affected by thermal loads which include the daily cycle, seasonal cycle and annual cycle. Thermal loads mode and thermal effects on bridges, especially for concrete girders, are quite essential but complicated. To investigate the temperature field and thermal stress in the thickness direction of a concrete box girder, the temperature field of a prestressed concrete continuous box girder bridge is monitored, and the temperature distribution in the thickness direction of the concrete box girder is analyzed. Finite element simulation, utilizing air elements specifically designed for concrete box girders, is employed to analyze the temperature field and thermal stress profiles along the thickness of the slab. The findings indicate a variation in temperature along the thickness of the concrete box girder slab. The most significant temperature differential, reaching up to 10.7 °C, is observed along the thickness of the top slab, followed by the bottom plate, with the web exhibiting relatively smaller differentials. Temperature in the full thickness range has a significant impact on the top plate, while the web plate and bottom plate are greatly influenced by temperature ranging from the outer surface to the center of the plate thickness. The temperature difference between the center of the plate thickness and the inner surface is approximately 0. The variation in temperature due to the variation in thickness direction is a temporal factor, wherein the outer layer of the roof is primarily compressed, while the inner layer is subjected to tension. The external surface of the web is mainly compressed. The stress exerted by the internal surface temperature is minimal. The internal and external surface effects of the floor are similar, and as time passes, tensile and compressive stresses appear.

Keywords: concrete box girder; temperature distribution; temperature effect



Citation: Shen, Q.; Chen, J.; Yue, C.; Cao, H.; Chen, C.; Qian, W. Investigation on the Through-Thickness Temperature Gradient and Thermal Stress of Concrete Box Girders. *Buildings* **2023**, *13*, 2882. <https://doi.org/10.3390/buildings13112882>

Academic Editors: Olga Szlachetka and Marek Dohojda

Received: 12 September 2023

Revised: 13 November 2023

Accepted: 15 November 2023

Published: 18 November 2023



Copyright: © 2023 by the authors. Licensee MDPI, Basel, Switzerland. This article is an open access article distributed under the terms and conditions of the Creative Commons Attribution (CC BY) license (<https://creativecommons.org/licenses/by/4.0/>).

1. Introduction

Solar radiation has an unavoidable impact on the integrity of concrete bridges in their natural habitat [1]. The bridge experiences a fluctuating and non-linear temperature field due to solar radiation. The temperature inside the concrete bridge has a major effect on the dependability and longevity of the concrete structure. The influence of temperature on concrete box girders is notably noteworthy [2–5]. Recent engineering research has revealed that in certain areas of box girders, temperature-induced stress surpasses that of vehicle load stress, leading to the primary cause of cracks. The fissures are highly conspicuous and have a propensity to progress even more [6,7].

The thermal and stress environments within concrete box girder bridges have been subjects of extensive research over an extended duration. In the past, accurately calculating the stress field solution in concrete box girder bridges was challenging due to the nonlinear and inhomogeneous distributions of the temperature fields. The thermal stresses are approximately computed employing the one-dimensional temperature gradient model as

outlined in the specifications. When the box girder structure is large or the environment is complex, it is inevitable that there will be differences with the actual temperature stress. Experiments were conducted to analyze the temperature variations in box girders, both horizontally and vertically. The study indicates that the temperature differences between the horizontal and vertical directions exert a significant influence on the strain of the box girder, while the temperature disparity between the horizontal and vertical orientations prominently impacts the web fracturing of the box girder [8]. Chen Hengye employed thermal transient analysis and thermal structure coupling technology to investigate the thermal balance of the Hangzhou Bay Sea-Crossing Bridge on the surface of the box girder. The study revealed that the temperature field outlined in the present specification not only fell short in its capacity to accurately predict the temperature-induced stresses within the concrete box girder but also failed to yield a reliable distribution law [9]. Chai Y.H. conducted a comprehensive analysis of the exact temperature distribution within a concrete box girder bridge located in California, USA, and juxtaposed it with the provisions outlined in AASHTO-2007 [10]. The findings indicated that the temperature difference was consistent within the roof's 0.4 m span, while outside this span, the temperature deviated from the prescribed standards. Oskar conducted an examination of the thermal characteristics of the Bridge, and ascertained that the temperatures of the web and bottom plate in the large-scale concrete box girder bridge exert a noteworthy influence on the thermal behavior of the box girder [11]. Taysi performed field observations and research on the temperature and stress fields of a prestressed concrete box girder bridge. His findings highlighted a safety deficiency in the analysis, stemming from the oversight of the temperature gradient in the bottom plate [12].

Currently, studies on concrete box girders both domestically and internationally are centering on the vertical gradient pattern and temperature influence. Researchers have largely disregarded the regional temperature distribution and the thickness of the bottom plate, web, and roof is affected by the local temperature [13,14]. The addition of the transverse stress caused by the longitudinal prestressed steel bars on the box girder section can lead to localized fractures in the girder. Hence, conducting further investigations to ascertain whether such oversights influence the overall thermal response of the box girder section would be of considerable value.

This study explores the temperature distribution along the vertical cross-section of various components within a bridge made of prestressed concrete box girder that can be found on a highway. These components include the top plate, bottom plate, and the web plate. The study subsequently formulates a finite element model to characterize the temperature field within the concrete box girder, drawing insights from observed temperature distributions. The temperature stress in the direction of plate thickness is calculated and analyzed. The temperature-induced stress in the plate thickness direction of the concrete box girder is considerable, thus necessitating further consideration in practical engineering.

2. Measurement, Results and Analysis of the Temperature Distribution in the Box Girder

2.1. The Layout of the Bridge, Information and Measuring Points

The special expressway bridge features a span configuration of 60 m + 100 m + 60 m, comprising a prestressed concrete continuous girder design that incorporates a single straight web box section within a single chamber. Due to the uniform temperature distribution throughout the cross-section of the box girder along the bridge, the side span Section 20 m distant from the side pier is chosen for temperature monitoring. The arrangement of specific measuring points is depicted in Figure 1.

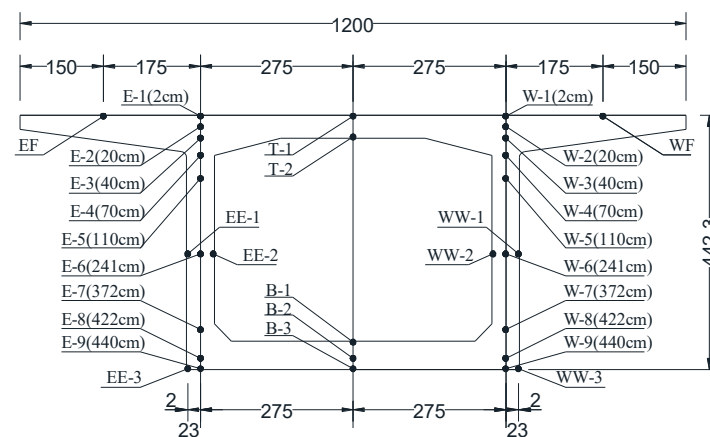


Figure 1. The layout of measuring points in a section.

2.2. Measurements, Results and Evaluation of the Thermal Field

The Lintong area of Xi'an experiences its highest annual temperature in July, which is a clear indication of the region's climate change. Consequently, July was chosen to conduct the temperature assessment of the concrete box girder.

The graph in Figure 2 shows the changes in temperature along the thickness of various sections of the concrete box girder. The temperature variations between the inner and outer surfaces of the top, bottom, and web sections of the concrete box girder depicted in the diagram exhibit a cyclical variation resembling a cosine function over time. The three demonstrate a simultaneous pattern of alteration, yet the top's temperature disparity attains its utmost magnitude initially in contrast to the temperature disparity between the web and the bottom plate.

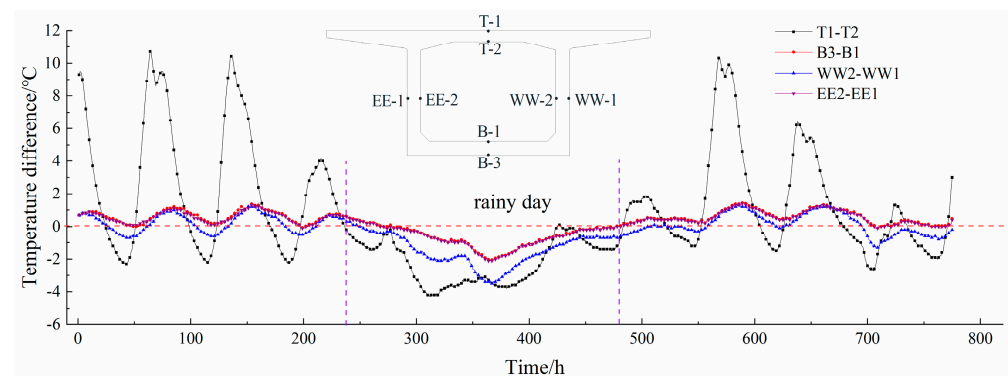


Figure 2. Temperature differences in the box girder plate versus time.

During daylight hours, the temperature disparities among the upper, lower, and webs are favorable, while during nighttime, they become unfavorable. When the sky is overcast and damp, the temperature difference between the inside and outside of the top and bottom plates can be significant, and the web is negative. When the ambient temperature experiences a significant decrease, the temperature within the enclosure exceeds that of the external environment, and heat primarily transfers from the interior to the exterior of the enclosure.

The temperature difference between the inside and outside of the upper plate is greatly affected by changes in the temperature of its environment. The greatest difference between positive and negative temperatures can be as high as 10.7 °C and 4.3 °C, respectively. The temperature difference between the interior and exterior surfaces of the web remains largely unaffected by fluctuations in ambient temperature. On the west web, the highest temperature variation is 1.3 °C and the lowest is 3.5 °C, while on the east web, the highest temperature variation is 1.4 °C and 2.1 °C, respectively. The ambient temperature has

minimal impact on the temperature disparity between the interior and exterior of the bottom plate. However, in the event of a sudden temperature decrease, a significant disparity arises between the interior and exterior of the bottom plate, characterized by a maximum positive temperature differential of 2°C and a maximum negative temperature differential of 2.5°C .

The temperature profiles of the concrete within the roof section of the concrete box girder are presented in Figure 3. Specifically, concrete temperature at a depth of 0.02 m beneath the roof surface exhibits daily fluctuations of approximately 13°C due to the influence of solar radiation. Additionally, Figure 3 illustrates that the temperature of concrete at a depth of 0.02 m above the lower surface of the roof experiences comparatively smaller daily variations. The roof experiences a decrease in temperature during nighttime or rainy days.

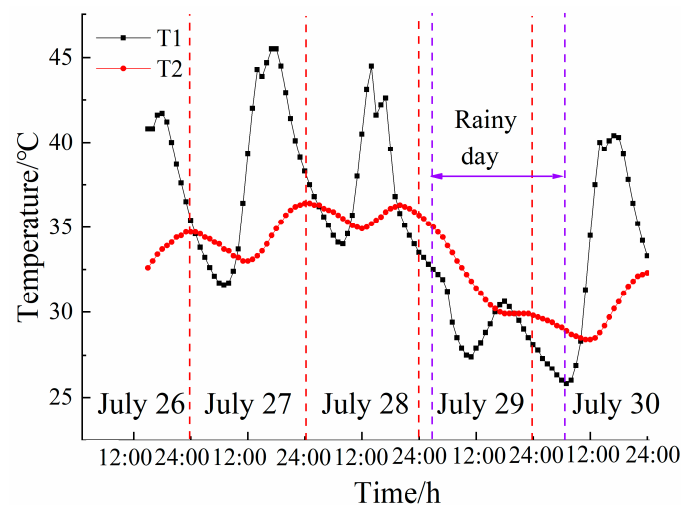


Figure 3. The temperature–time curve of the concrete in the top slab of the box girder.

The temperature distribution within the concrete box girder section's east and west web elements is illustrated in Figure 4. The concrete temperature at a depth of 0.02 m from the outer surface of the east and west webs has a large temperature fluctuation in one day, and the fluctuation value is approximately 3°C close to the web, due to the influence of solar radiation and sunset cooling. The temperature of the concrete on the inner surface changes a lot every day. The temperature of the web varies depending on the thickness of the plate, with a positive difference during the day and a negative difference at night, and there is a noticeable temperature difference along the web thickness. The east and west webs have the same temperature distributions, and the change trend is similar.

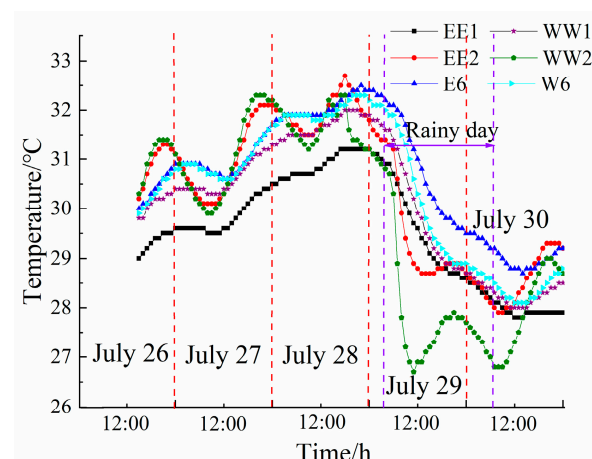


Figure 4. Time records of temperature of concrete in the east and west webs of the box girder.

An illustration of the temperature distribution in the concrete at the lower plate of the concrete box girder section can be seen in Figure 5. The bottom plate concrete has a lower temperature compared to the web concrete. With the exception of rainy days, the temperature on the bottom plate of the concrete box girder is equivalent to the negative temperature at the plate's thickness. During periods of clear weather or when the temperature rises, a significant variation in temperature can be observed along the breadth of the bottom plate.

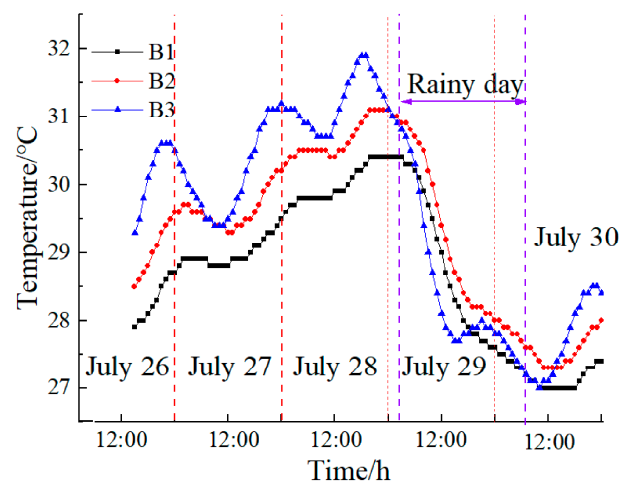


Figure 5. The temperature–time curve of the concrete in the bottom slab of the box girder.

In order to conduct a more in-depth analysis of the temperature gradient distributions in the wall thickness direction of the roof, web, and bottom plate, temperature sample data from 17 July 2021 (rainy day) and 20 July 2021 (sunny day) were chosen as the subjects for analysis.

The temperature gradient along the web wall thickness direction is illustrated in Figure 6. The highest difference between positive and negative temperatures is 1.3 °C and 3.5 °C, respectively. The variation in temperature and the disparity in temperature are more pronounced in areas nearer to the outermost layer of the internet. The temperature gradient exhibits a linear variation extending from the outer surface of the web to a distance of 23 cm inward from the web's outer surface. From the innermost layer of the web to the outermost layer 23 cm away, the temperature fluctuates gradually, and the temperature difference is nearly negligible. When a positive temperature difference is observed, the disparity in temperature between the outer surface of the web and the center of the web wall thickness surpasses that observed when subjected to negative temperature variations. The variation in temperature along the web's thickness spans from the outer surface to the web's center. Furthermore, the temperature variation in the web's thickness at 14:00 is less pronounced than at 19:00, suggesting that during summer, the edge plate's shielding properties prevent the web from being directly exposed to sunlight, even under high levels of solar radiation. During the summer months, the flange plate provides shade to the concrete box girder's web, resulting in a slight variation in temperature along the plate's thickness. Despite the cooling effect on rainy days, the web experiences a significant decrease in temperature as it moves along the plate thickness. Inside and outside the plate, there exists a variation in lateral temperature ranging from −3.5 °C to 1.3 °C. The analysis indicates that the threshold at which the temperature of the web undergoes a significant change is roughly 0.25 cm away from the outer surface of the web.

Figure 7 illustrates the variation in temperature along the lower plate of the concrete box girder. The bottom plate exhibits a vertical temperature differential akin to the lateral temperature gradient of the web, with a peak positive temperature differential of 1.5 °C and a maximum negative temperature difference of 2 °C. The temperature gradient between the outer surface and the inner surface of the bottom plate exhibits a linear variation, with

the inner surface of the bottom plate undergoing minimal changes within a 20 cm distance from the outer surface, resulting in an almost imperceptible temperature differential. The variation in temperature is roughly proportional to the plate's thickness.

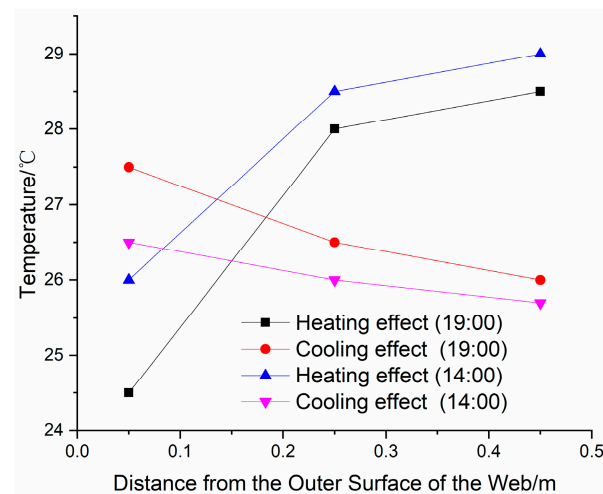


Figure 6. Temperature distribution in the direction of the web's thickness.

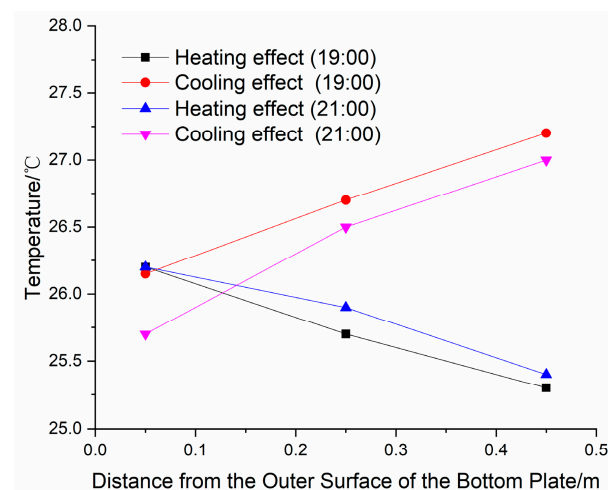


Figure 7. Temperature distribution in the direction of the bottom slab's thickness.

On 13 July, a sunny day, the roof exhibited its highest positive temperature difference, while on 17 July, a rainy day, it displayed its highest negative temperature difference. These data points were both employed to investigate the temperature distribution across the thickness direction of the roof.

The graph presented in Figure 8 illustrates a pronounced temperature variation within the roof, particularly along the direction of plate thickness. Notably, significant temperature discrepancies, both positive and negative, are observed near the outer surface of the roof, spanning its entire thickness. The temperature delta between the interior and exterior surfaces of the roof can attain a maximum of 10.7 °C, with the highest temperature differential between both sides reaching up to 4.3 °C. The disparity in temperature between the interior and exterior of the roof can lead to significant temperature strain and even fracture the structure. It is essential to examine the temperature distribution properties of the box girder along the beam height direction and contemplate how the temperature distribution across the thickness of the roof plate influences the temperature distribution profile in the beam direction of the box girder. This is particularly crucial due to the significant fluctuations in roof temperature along the thickness of the plate and the substantial temperature difference.

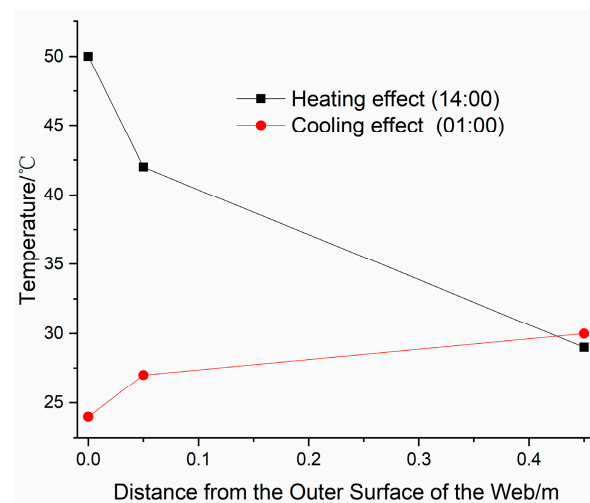
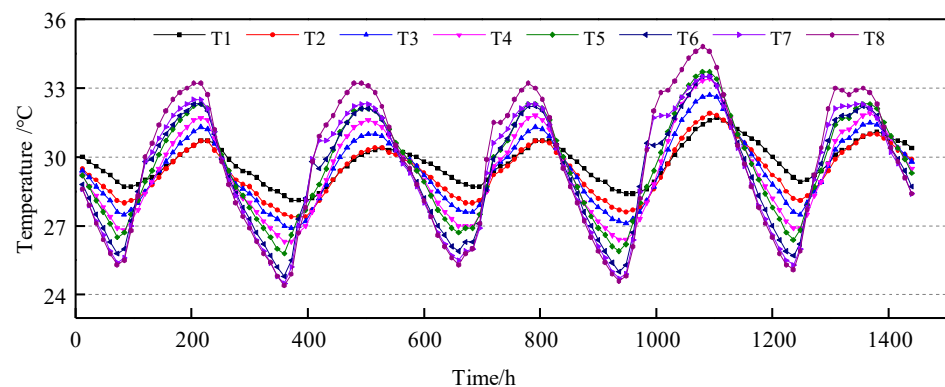
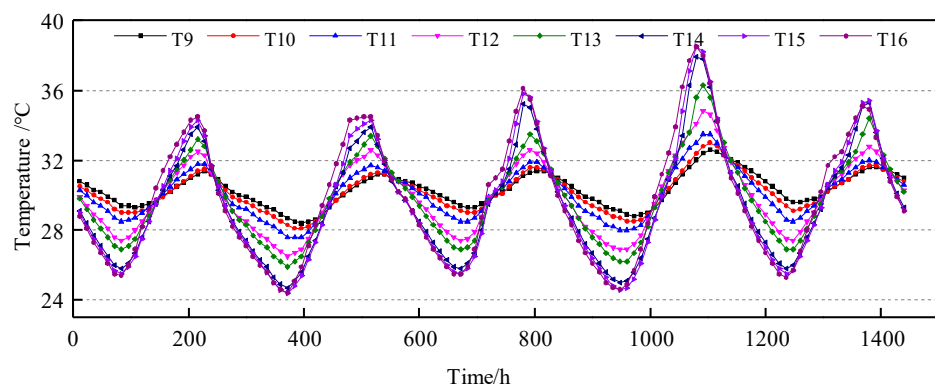


Figure 8. Temperature distribution in the direction of the top slab's thickness.

Examine the summer temperature distribution attributes of the box girder by considering the temperature–time profile of the box girder during the five days preceding and following the 2017 summer solstice as the subject of investigation. The temperature–time curves of the box girder's right measuring points T1~T8 during the five days before and after the summer solstice in 2017 are depicted in Figure 9a. The temperature–time profiles for measuring points T9~T16 of the box girder during the five days before and after the summer solstice in 2017 are depicted in Figure 9b.



(a)



(b)

Figure 9. (a) Temperature time profile of the right measurement point. (b) Temperature time profile of the left measurement point of box girder.

It is evident from the illustration that The box girder's temperature experiences the combined influence of solar radiation and diurnal temperature changes over a span of five days, leading to noticeable variations at each measurement point. The cross-sectional temperature variation exhibits the following attributes:

- (1) When comparing the temperature change amplitude at each measurement point, it is evident that the temperature change amplitude at the bottom plate surpasses that at the top plate, and the closer it gets to the bottom plate, the more pronounced the temperature change amplitude.
- (2) The contrast between the vertical negative temperature gradient and the upward vertical temperature gradient is more pronounced, with the vertical positive temperature gradient in the background bridge manifesting during the night and morning when the box girder's temperature was lower, while vertical negative temperature gradient manifesting during the day when the railroad box girder's temperature was higher. Incorporation of ballast and concrete bridge panels atop the railway box girder deck, in conjunction with the presence of 3-m-high side guardrails flanking the box girder bridge, effectively shields the bridge deck from diurnal solar exposure. This arrangement directs sunlight exclusively onto either side of the box girder belly plate. In the realm of structural engineering, it is imperative to acknowledge that the relative proximity of the web plate to the bottom plate significantly influences the duration of direct solar irradiation, giving rise to a vertical adverse temperature gradient, wherein the temperature recorded at measurement locations on the upper plate is less than that observed on the lower plate. The ballast and concrete bridge panels' covering effect causes the top plate to dissipate heat at a slower pace compared to the bottom plate and belly plate during the night. The top plate temperature is higher than the bottom plate temperature, resulting in a vertical positive temperature gradient.
- (3) In the realm of bridge engineering, it is observed that the temperature change in the lower plate manifests itself prior to the temperature variation in the upper plate. Moreover, the proximity of the lower plate to its designated position correlates with an earlier onset of temperature alteration. At 5:35 in the morning of the summer solstice, the sun ascends from the ground plane, radiating its rays directly onto the right web of the box girder, with a height of 4.8 m. Subsequently, the height of the direct solar radiation on the web gradually diminishes, and the closer it gets to the bottom plate, the more it is affected by it; the temperature of the bottom plate is lower than that of the top plate in the morning, indicating a thermal gradient. As time passes, the box girder's cross-section temperature decline process causes solar radiation to lose its role in maintaining a higher temperature in the bottom plate position. The temperature of the bottom plate started to decrease as soon as possible.

Examine the disparity in temperature between the left and right sides of the box girder over the five days prior to and following the summer solstice, three sets of measurement points near the middle of the top plate, bottom plate and web plate were chosen to compare the temperature time course curves of the two sides, as illustrated in Figure 10.

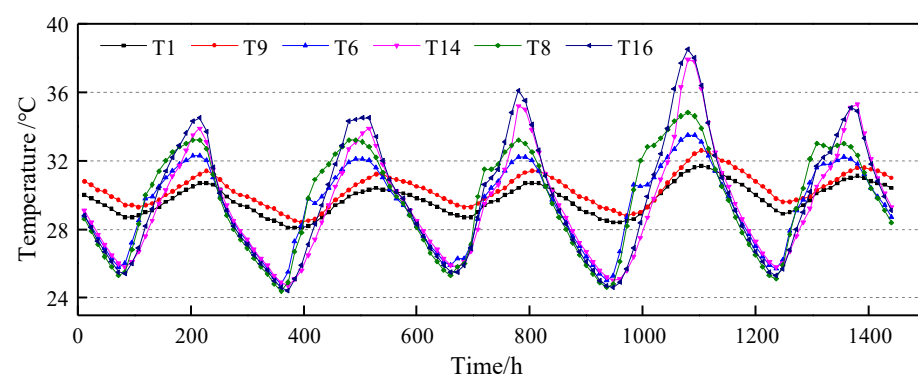


Figure 10. Comparison of temperature time course curves between left and right sides of box girder.

In order to facilitate our description, the transverse temperature difference is ascertained by calculating the temperature differential between measurement points situated on the top and bottom plates on the left and right sides, respectively. In cases where the temperature at the left measurement point is lower than that at the right measurement point, the transverse temperature difference is denoted as a positive value. Conversely, when the temperature at the right measurement point exceeds that at the left measurement point, the transverse temperature difference is represented as a negative value (the negative temperature difference having a negative numerical value).

Examining the temperature–time curves on both sides of the box girder, the following deductions can be made.

- (1) The uppermost plate of the box girder shows minimal fluctuation in transverse temperature, while the lower plate showcases a more noticeable disparity in transverse temperature. In the initial and intermediate stages of the box girder temperature rise, there is a noticeable increase in transverse positive temperature, followed by a decrease in transverse negative temperature before and after the peak value.

In spite of the higher temperature recorded at measurement point T9 on the left side of the box girder in comparison to measurement point T1 on the right side of the girder, the differential temperature gap between T9 and T1 has consistently remained within a narrow margin, consistently measuring less than 1 °C. Furthermore, the lateral temperature differential across the top plate remains relatively insignificant. When the daily temperature of the box girder fluctuates near the peak and valley, the temperature values of measuring point T14 on the left web are similar to those of measuring point T6 on the right web, while the temperature values of measuring point T16 on the left bottom plate and measuring point T8 on the right bottom plate are similar. The bottom plate exhibits a substantial disparity in lateral temperature. As the temperature of the box girder increases, it appears that the right side of the temperature change occurs sooner than the left side of the temperature change, resulting in a more pronounced transverse positive temperature difference. Subsequently, owing to the rapid escalation of temperature along the left side, the temperature reading at measurement point T14 on the left side of the web plate steadily converges with and ultimately surpasses the temperature value at measurement point T6 on the right side of the web plate. Simultaneously, in a progressive manner, the temperature at measurement point T16 on the left side of the bottom plate gradually approaches and eventually exceeds that of measurement point T8 on the right side of the bottom plate, resulting in a transverse negative temperature differential across the bottom plate. When the daily temperature of the box girder is close to its highest point, the lateral temperature of the bottom plate of the box girder has decreased significantly. As the temperature inside the box girder dropped, the temperature recorded at position T14 on the left web progressively approached that of measurement point T6 located on the right web. The temperature at point T16 on the left bottom plate gradually neared the temperature at point T8 on the right bottom plate simultaneously. The box girder bottom plate's lateral negative temperature difference gradually diminished until it ceased to exist. The bottom plate of the box girder remained relatively stable until the daily temperature fluctuation neared the peak valley.

- (2) The right side experiences an earlier temperature change compared to the left side at the identical transverse position.

Examine and contrast the sequence of temperature fluctuations at the left and right measuring points positioned horizontally, with the top plate measurement point T1 experiencing an earlier temperature change compared to the top plate measurement point T9, the web measuring point T6 displaying an earlier temperature change compared to the web measuring point T14, and the bottom plate measuring point T8 displaying an earlier temperature change compared to the bottom plate measuring point T16. At 5:35 a.m. on the summer solstice, the sun ascends from the ground plane, illuminating the right side of the box girder and subsequently the left side as time elapses; there is a temporal precedence in the temperature fluctuation observed on the right side compared to the left side of the box

girder. This phenomenon can be attributed to the sun's trajectory, as it moves across the sky from the left side of the box girder, causing the left side to be directly exposed to solar radiation while the right side remains shielded from direct solar radiation. This differential exposure results in a discernible temperature gradient between the right and left sides.

(3) The bottom plate will experience both vertical and lateral temperature effects simultaneously.

The analysis of Figures 9 and 10 reveals that the box girder temperature experiences fluctuations during the day following the initial temperature increase. This led to a substantial increase in temperature and the existence of a bottom plate in the difference between transverse positive temperatures. When the box girder is close to the highest point of its daily temperature variation, the top and bottom plates of the box girder will have a large vertical temperature difference, and the bottom plate will also have a large transverse temperature difference.

3. Simulation of the Temperature Field of the Concrete Box Girder Section

3.1. Temperature Field Boundary Conditions

Concrete box girders exposed to sunlight experience the predominant influences of three primary factors: solar radiation, convective thermal exchange, and radiative thermal transmission. Therefore, the temperature distribution within the concrete box girder can be determined by implementing prescribed boundary conditions [15]. The thermal flux density at the junction of the concrete box girder is:

$$q = q_s + q_c + q_r \quad (1)$$

The thermal flux density of solar radiation is denoted by q_s , whereas the thermal flux density of convective thermal exchange is represented by q_c , and q_r is the thermal flux density of radiative thermal transmission.

Solar radiation encompasses direct solar radiation, solar scattering and ground reflection, and the thermal flux density associated with solar radiation can be formulated as follows:

$$q_s = \alpha(I_{D\phi} + I_{d\beta} + I_f) \quad (2)$$

where $I_{D\phi}$ is the coefficient related to the absorption of radiation on the exterior surface of the concrete box girder, with values falling within the range of 0.50 to 0.70 [13]. $I_{d\beta}$ is solar scattered radiation intensity, and I_f is the ground reflection intensity. The specific calculation can be found in the literature [14,15].

The process of energy exchange between the fluid in contact with the concrete box girder's surface and the box girder itself are known as convective thermal exchange, and the thermal flux density of convective heat transfer can be calculated as follows:

$$q_c = h_c(T_a - T) \quad (3)$$

where T_a is ambient atmospheric temperature, T is the box girder structure temperature, and h_c is the convective heat transfer coefficient, which is usually determined by experiment or experience as follows:

$$q_c = 4a + 5.6, v \leq 5 \text{ m/s};$$

$$q_c = 7.15v^{0.78}, v > 5 \text{ m/s}$$

The value of v represents the velocity of the wind.

The radiative heat transfer for concrete box girders can be calculated using the following equation:

$$q_r = h_r(T_a - T) - q_{ra} \quad (4)$$

$$h_r = C\varepsilon[(T + 273)^2 + (T_a + 273)^2](T + T_a + 546) \quad (5)$$

$$q_{ra} = \frac{1 + \cos(\beta)}{2}(1 - \varepsilon_a)\varepsilon C(273 + T_a)^4 \quad (6)$$

The radiative heat transfer coefficient is denoted by h_r ; q_{ra} corresponds to the sloping sky radiation effect; ε_a denotes the atmospheric radiation coefficient, with a value of 0.82; C is the Stefan–Boltzmann constant, taking $5.67 \times 10^{-8} \text{ W} \cdot \text{m}^{-2} \cdot \text{K}^{-4}$; and ε is the emissivity of the object, taking 0.85 to 0.95.

3.2. Model Parameter Values and Finite Element Simulation

To be specific, the solar radiation absorption rate at the concrete box girder surface is 0.6, and the thermal characteristics of the concrete are detailed in Table 1.

Table 1. The thermal characteristics of the concrete.

Material	Density (g/cm ³)	Thermal Conductivity (J·m ⁻¹ ·°C ⁻¹)	Specific Heat Capacity (J·kg ⁻¹ ·°C ⁻¹)
C50 Concrete	2500	0.75	10.10

This study employs finite element simulation to replicate the temperature field, aiming to evaluate the impact of temperature loading on the thermal properties of concrete box girder sections. Subsequently, the simulation results are cross-referenced with experimental data to validate their accuracy. Following this validation, a study is carried out to examine the thermal impact on the box girder section.

The finite element software ABAQUS (Version 6.13 2021) is used to establish a box girder segment model for conducting a momentary examination of the temperature field and temperature-induced self-stresses, as illustrated in Figure 11. Initially, a linear heat transfer element consisting of eight nodes DC3D8 was utilized to simulate the heat transfer within the concrete box girder. Subsequently, this eight-node linear heat transfer element DC3D8 was transformed into an eight-node linear hexahedral element C3D8R for conducting structural analysis and calculations.

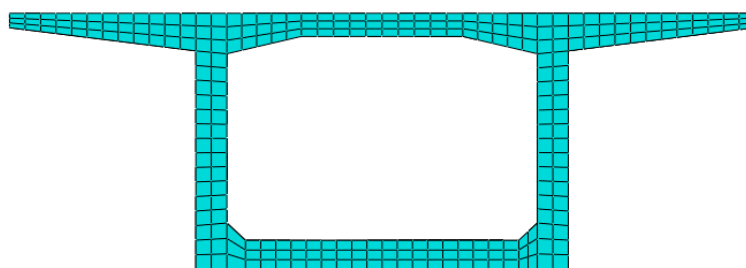


Figure 11. A representation of the finite element structure of a concrete box girder.

The period of clear weather from 10 July 2021 to 13 July 2021 is selected as the calculation time. The first three days are the transition time to obtain an accurate temperature field, and 13 July is the time for the simulation and analysis of the temperature field.

Through finite element analysis, the temperature distribution at various time instances for the box girder can be determined. Figures 12–14 depict the temperature–time profiles of the measured and calculated temperature data at various points along the thickness direction of the top plate, web plate, and bottom plate of the section.

As illustrated in Figures 12–15, the calculated temperatures align closely with the measured values, displaying consistent temperature distributions with variations within 1 °C. The box girder’s section experiences an uneven temperature field due to solar radiation. Notably, the upper edge of the top plate exhibits significant temperature fluctuations, with temperatures beginning to rise at 8:00 and reaching their daily peak at 18:00. The web and bottom plate outer surfaces display minimal temperature variations, while the internal temperature changes gradually. The box girder section is vertical in height, the top plate experiences dramatic temperature fluctuations, the bottom plate shows minor temperature changes, and the web plate remains relatively stable with minimal temperature variation.

This indicates that the finite element model accurately captures the genuine temperature field of the box girder section.

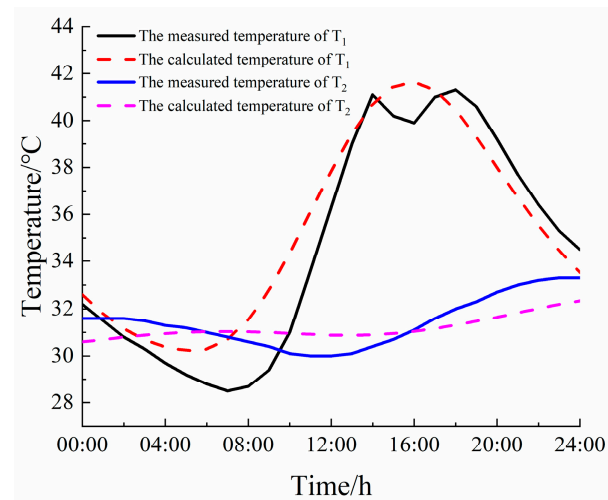


Figure 12. Temperature time curve for measuring and calculating roof temperature.

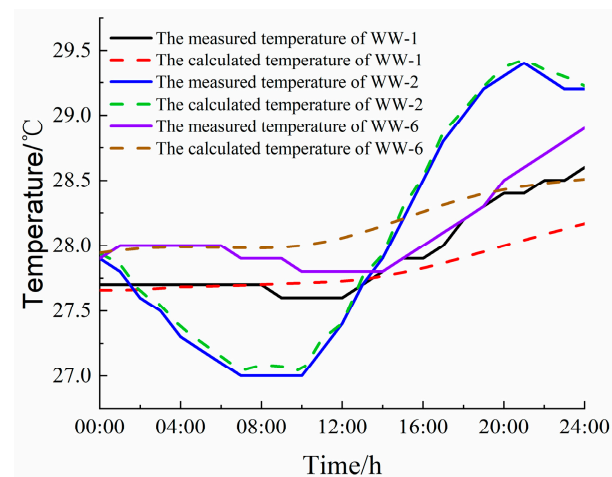


Figure 13. Temperature–time profiles for measuring and calculating web temperatures.

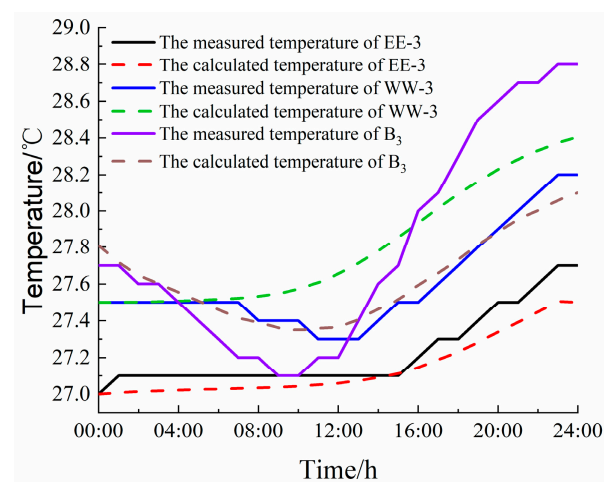


Figure 14. Temperature–Time Profiles for Measured and Calculated Bottom Plate Temperatures.

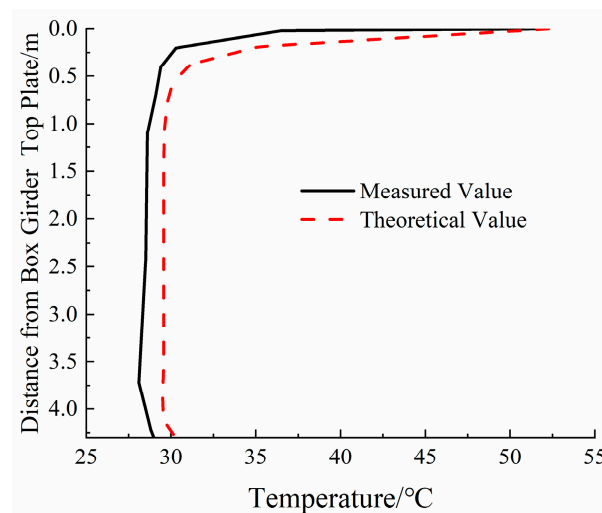


Figure 15. Measured and Calculated Temperature Distribution Along the Height Direction of the Beam.

4. Analysis of Self-Stress and Section Temperature

4.1. Diurnal Temperature Stress Change in a Section

Induced heat loads exhibit noticeable variations with changing solar radiation intensity. Consequently, the central positions of the exterior and interior of the concrete box girder were selected to analyze the daily thermal stress, as shown in Figure 16.

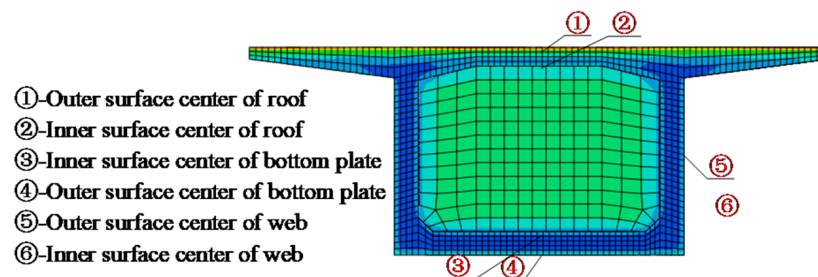


Figure 16. Parts of thermal stress analysis.

Figure 17 illustrates the daily variation in temperature-induced self-stress on the upper and lower edges of the concrete box girder's top plate. The top plate experiences substantial temperature stress fluctuations due to direct solar radiation, resulting in significant thermal stress changes. Starting from 8:00, the highest point of the upper plate exhibits compressive stress, which gradually intensifies. By 14:00, the compressive stress reaches its peak at -8.5 MPa. Subsequently, the compressive stress on the upper edge diminishes and transitions into tensile stress. By 24:00, the tensile stress at the bottommost part of the upper plate reaches its maximum at 1.8 MPa. Conversely, the bottommost part of the upper plate endures tensile stress throughout the day, steadily increasing from 8:00 and peaking at 4.7 MPa by 15:00, followed by a gradual reduction. At 24:00, the tensile stress at the lower edge aligns with that at the highest point of the upper plate.

Figure 18 shows the diurnal variation of temperature self-stress at the center of both the inner and outer surfaces of the bottom plate. It is observed that the temperature stress at the center of the bottom plate surface changes approximately as a cosine curve with time. The center of the upper and lower surfaces of the bottom plate is under compressive stress from 8:00 to 19:00 and tensile stress at other times. The maximum compressive stress at the upper edge of the bottom plate is 0.95 MPa, and at the lower edge, it reaches a maximum of 0.68 MPa, with both peaks occurring at 13:00. The maximum tensile stresses on the upper and lower edges of the bottom plate are 0.84 MPa and 0.51 MPa, respectively, and both are observed at 1:00.

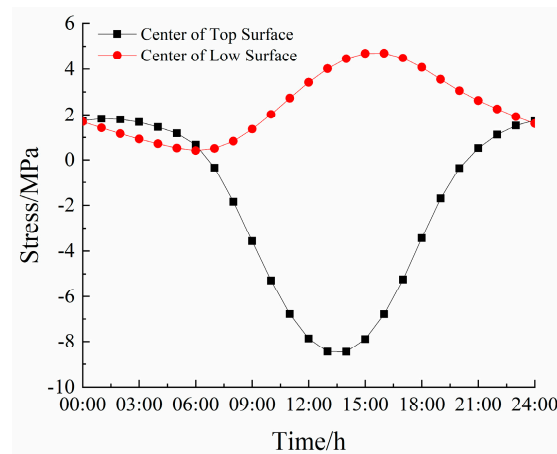


Figure 17. Time record of stress for the inner and outer surfaces at the center of the top plate.

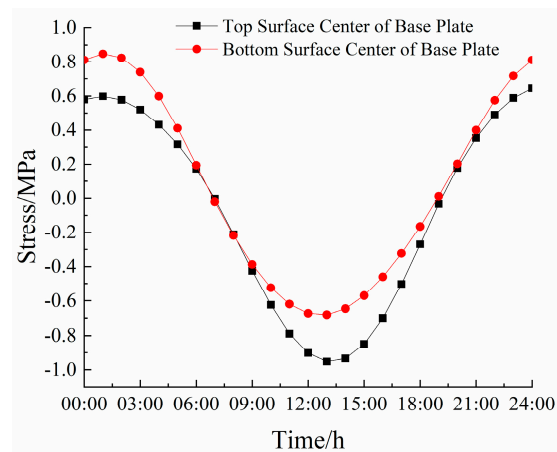


Figure 18. Time records of the central stress on the inner and outer surfaces of the bottom plate.

Figure 19 depicts the daily variations in temperature-induced stress at the center of the inner and outer surfaces of the web. Notably, there is a considerable disparity in temperature-induced stress between the inner and outer surface centers, with the conditions at the outer surface center being less favorable. The inner surface center of the web experiences compressive stress throughout the day, albeit with a gradual change. The maximum compressive stress recorded is 0.73 MPa. The temperature stress time record at the center of the outer surface of the web is similar to a sine curve. The tensile stress is very small, but the compressive stress can reach a maximum of 4.2, with a larger magnitude.

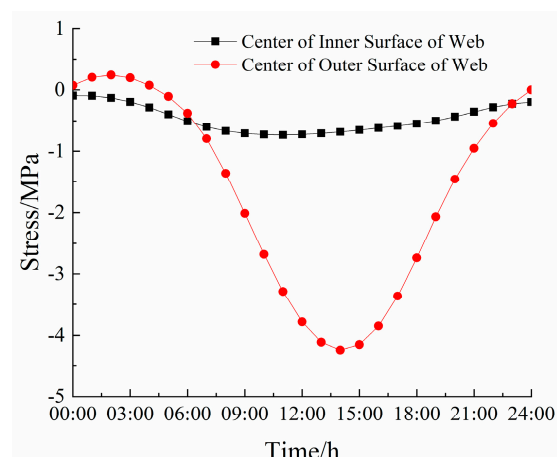


Figure 19. Time record of central stress on inner and outer surfaces of the web.

4.2. Stress Distributions on the Inner and Outer Surfaces of the Plate Thickness

The lateral distribution of temperature-induced stress along the inner and outer surfaces of the top plate is depicted in Figure 20. The center of the box girder is the most critical stress location for the top plate, as illustrated in Figure 1. Under the most daily unfavorable temperature load, the upper edge of the top plate experiences a maximum compressive stress of 8.5 MPa and a maximum tensile stress of 1.5 MPa. When subjected to a negative temperature gradient, the upper edge of the top plate consistently experiences tensile stress, with relatively uniform tensile stress values. Conversely, under the influence of a positive temperature gradient, the upper edge of the top plate is consistently under compressive stress, with compressive stress gradually decreasing from the box girder's center towards the flange plates. The temperature-induced stress on the lower edge of the top plate gradually transitions from tensile stress at the center of the box girder to compressive stress on both sides of the flange plates.

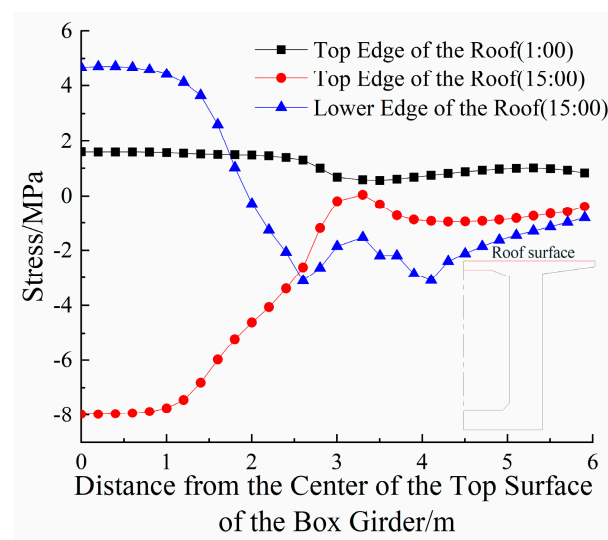


Figure 20. Stress distributions on the inner and outer surfaces of the top plate.

Figure 21 illustrates the lateral distribution of temperature-induced stress on the inner and outer surfaces of the bottom plate. Notably, the temperature-induced stress on both the upper and lower surfaces of the bottom plate exhibits a symmetrical distribution. Under the influence of the most unfavorable daily temperature load, the temperature stress on the inner and outer surfaces of the bottom plate is generally uniform, except for a notable reduction in stress at the junction between the bottom plate and the web. The center of the box girder is the most critical stress location on the bottom plate surface. In the presence of a positive temperature gradient, the inner surface experiences compression, while the outer surface experiences tension, resulting in maximum tensile and compressive stresses of up to 1 MPa. Conversely, with a negative temperature gradient, the inner surface of the bottom plate experiences tensile stress, while the outer surface experiences compressive stress, with maximum tensile and compressive stresses also reaching 1 MPa.

Figure 22 shows the distributions of temperature stress along the inner and outer surfaces of the web. The outer surface of the web experiences a more pronounced impact from temperature loading compared to the inner surface. Notably, the stress at the intersection of the web's outer surface and the stem undergoes a sudden transformation. The temperature stress gradually decreases along the inner and outer surfaces of the web, starting from the top plate and extending to the bottom plate, under both positive and negative temperature gradients. This observation highlights the proximity of the top plate and the web to the primary stress points on both the inner and outer surfaces of the web.

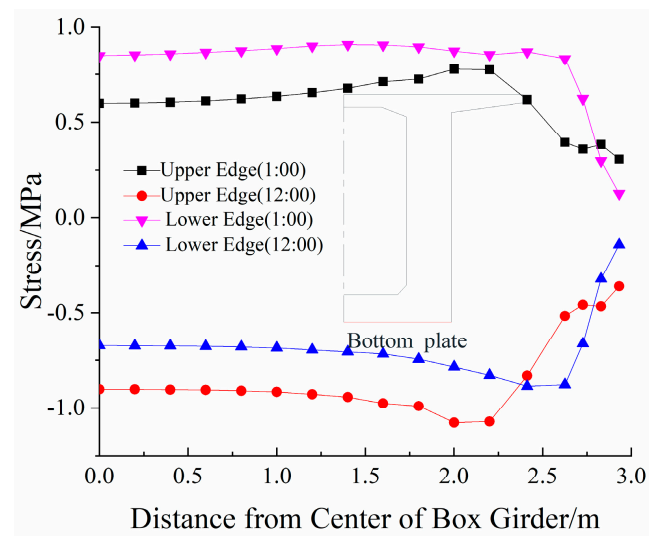


Figure 21. Stress distributions on the inner and outer surfaces of the bottom plate.

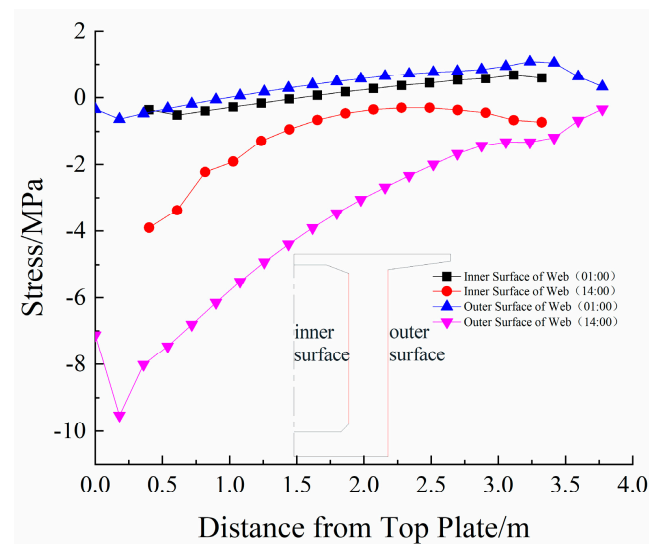


Figure 22. Stress distributions on the inner and outer surfaces of the web.

4.3. Stress Distributions along the Thickness Direction of the Section Plate

The temperature transfer in the thickness direction varies across the top plate, bottom plate, and web of the box girder. There is a disparity between the internal stress in the direction of plate thickness and the surface stress. Hence, it is crucial to examine the dispersion of temperature-induced stress in the direction of plate thickness. Figure 23 illustrates the distribution of stress along the thickness of the top plate. Compared with the internal temperature stress in the thickness direction of the top plate, the temperature stress on the inner and outer surfaces of the top plate is maximal, displaying distinct time-dependent characteristics. During daytime, the outer surface of the top plate undergoes a shift in temperature stress, transitioning from compressive to tensile stress, with the reverse occurring at night. Along the vertical direction of the top plate, the diurnal variation in the temperature stress is different, and the temperature stress varies greatly during the day. The maximum variation occurs at 14:00. The compressive stress on the outer surface gradually diminishes from 8.5 MPa to 0 MPa at position 1/3 from the top plate's outer surface. Then, the temperature stress is converted into tensile stress and then gradually increases. The maximum tensile stress at the inner surface of the top plate is 4.5. The variation in temperature stress at night is small. This is because the temperature gradient distribution inside the top plate is different during the day and night, which makes the

stress distribution different in the daytime and at night. The top plate experiences direct sunlight exposure during the day, resulting in significant temperature fluctuations, whereas at night, in the absence of light exposure, temperature variations are gradual.

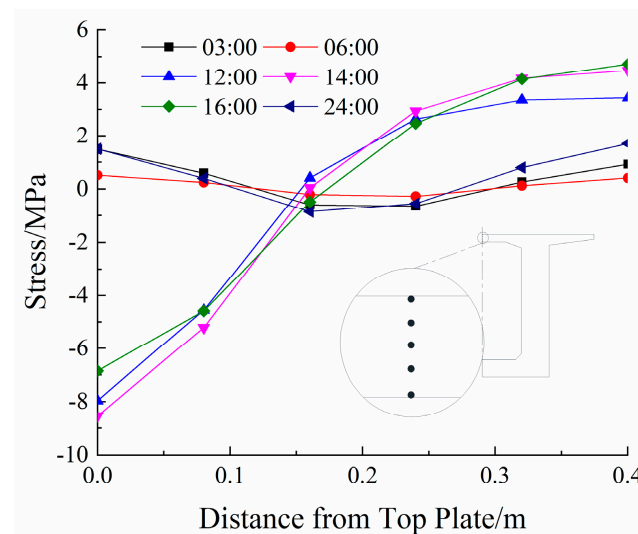


Figure 23. Stress distribution along the thickness of the top plate.

Figure 24 depicts the distribution of temperature-induced stress in the direction of the bottom plate's thickness. The temperature-induced pressure on the bottom plate's thickness can be considered to be approximately symmetrically distributed during the day and night. Commencing at the outermost layer of the bottom plate and extending up to a distance of 0.2 m from the outermost layer of the bottom plate, the maximum compressive stress decreases linearly to 0 MPa in the daytime and increases linearly with the same slope as the maximum tensile stress. At night, the maximum tensile stress decreases linearly to 0 MPa and increases linearly with the same slope as the maximum compressive stress. The trends exhibit a contrasting pattern between the outer and inner surfaces of the bottom plate, spanning a distance of 0.3 m. Within the range from 0.2 m to 0.3 m from the outer surface of the bottom plate, the temperature stress changes slightly during the day and night and can be considered to remain unchanged.

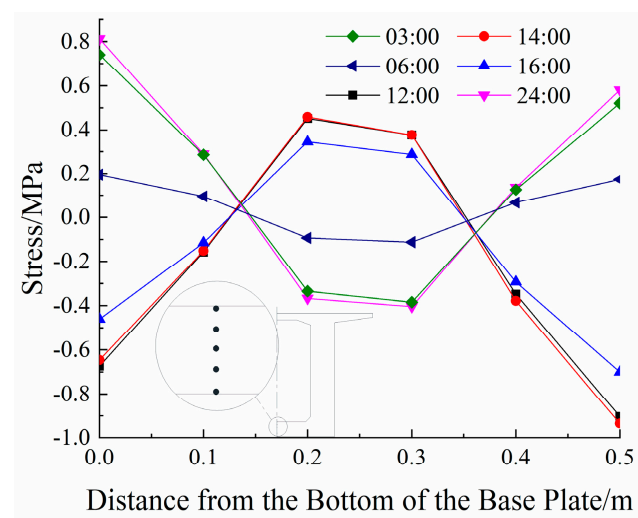


Figure 24. Stress distributions along the thickness of the bottom plate.

5. Conclusions

By analyzing the temperature data of the prestressed concrete continuous box girder bridge and conducting simulation calculations on the temperature field of the box girder, this research looks into how the temperature field affects the thickness of the concrete box girder and how it is distributed. The key findings are as follows:

- (1) Along the thickness direction of the concrete box girder, there exists a temperature gradient. The maximum temperature gradient occurs along the top plate thickness direction, reaching a maximum value of up to 10.7 °C. The gradient is somewhat smaller in the bottom plate, and even smaller in the web. There are temperature difference changes in the full range of the top plate thickness direction. The web and the bottom plate at the center of the outer surface plate thickness exhibit a disparity in temperature. There is an approximate temperature difference of 0 between the center of the plate thickness and the inner surface of the web.
- (2) The concrete box girder's top surface is subjected to considerable temperature-induced stress, reaching a maximum compressive stress of 8.5 MPa and a maximum tensile stress of 1.5 MPa. The temperature pressure stress on the outer surface of the web is 4.0~8.0 MPa, the temperature stress on the inner surface is smaller than that on the outer surface, and the temperature stress on both the inner and outer surfaces of the bottom plate is less than 1 MPa.
- (3) The top plate experiences significant fluctuations in temperature stress as it moves along its thickness. The inner and outer surfaces experience the most significant temperature stresses, which gradually diminish as the plate thickness increases. The distribution of temperature stress along the thickness direction of the bottom plate can be regarded as approximately symmetrical throughout the day and night.
- (4) With the increase in thickness, the standard value of positive temperature difference decreases, the standard value of negative temperature difference increases, and the thermal stress is proportional to the gradient of thickness direction.

Author Contributions: Methodology, W.Q.; Validation, C.Y.; Investigation, Q.S.; Resources, Q.S. and W.Q.; Data curation, J.C. and C.Y.; Writing—original draft, H.C.; Writing—review & editing, J.C.; Visualization, J.C. and C.C. All authors have read and agreed to the published version of the manuscript.

Funding: This work was supported by the National Natural Science Foundation of China (Grant No. 52208395), the Nantong Science and Technology Plan Project (Grant Nos. JC2021169 and MS22022067), and the Large Instruments Open Foundation of Nantong University (Grant No. KFJN2260). The authors appreciatively acknowledge the financial support of the abovementioned agencies.

Data Availability Statement: The data used to support the findings of this research are available from the corresponding author upon request. The data are not publicly available due to privacy.

Conflicts of Interest: The authors declare no conflict of interest.

References

1. Lei, X.; Ye, J.; Wang, Y. Representative value of solar thermal difference effect on PC box-girder. *J. Southeast Univ.* **2008**, *38*, 5–9.
2. Lei, X.; Ye, J.; Wang, Y. Analysis of concrete box-girder temperature and strain based on long term observation. *J. Jiangsu Univ. Nat. Sci. Ed.* **2010**, *31*, 230–234, 239.
3. Elbadry, M.M.; Ghail, A. Temperature variations in concrete bridges. *J. Struct. Eng.* **1983**, *109*, 2355–2374. [[CrossRef](#)]
4. Saetta, A.; Scotta, R.; Vitaliani, R. Stress analysis of concrete structures subjected to variable thermal loads. *J. Struct. Eng.* **1995**, *121*, 446–457. [[CrossRef](#)]
5. Han, D.; Tan, Y. Temperature variation in pre-stressed concrete single-cell box-girder bridges. *J. Sichuan Univ. Eng. Sci. Ed.* **2008**, *40*, 7–13.
6. Mirambell, E.; Aguado, A. Distribution of temperature and stress in concrete box girder bridge. *J. Struct. Eng.* **1990**, *116*, 2388–2409. [[CrossRef](#)]
7. Liu, Y.; Chen, X. Research on box girder temperature field using artificial neural network. *China J. Highw. Transp.* **2000**, *13*, 69–72.
8. Emerson, M. Bridge Temperatures for setting bearings and expansion joints. *TRRL Lab. Rep. (Transp. Road Res. Lab. Great Br.)* **1979**, *5*, 21–28.

9. Chen, H.; Xie, X.; Zhang, Z. Temperature Field and Stress Field of Prestressed Concrete box girder bridge. *J. Zhejiang Univ. (Eng. Sci.)* **2005**, *39*, 85–90. [[CrossRef](#)]
10. Chai, Y.H. Temperature Gradients in lightweight aggregate concrete box-girder bridges. *J. Part A Civ. Struct. Eng.* **2013**, *6*, 199–210. [[CrossRef](#)]
11. Oskar, L.; Sven, T. Estimating extreme values of thermal gradients in concrete structures. *Mater. Struct.* **2011**, *44*, 1491–1500.
12. Taysi, N.; Abid, S. Temperature distributions and variations in concrete box-girder bridges: Experimental and finite element parametric studies. *Adv. Structural Eng.* **2015**, *18*, 469–486. [[CrossRef](#)]
13. Zhang, H.; Wu, E.-J. Statistical model estimation of extreme temperature gradient of long-span bridges combined parameter updating. *Eng. Mech.* **2017**, *34*, 124–130.
14. Rodriguez, L.E.; Barr, P.J.; Halling, M.W. Temperature Effects on a Box-Girder Integral-Abutment Bridge. *J. Perform. Constr. Facil.* **2014**, *28*, 583–591. [[CrossRef](#)]
15. Lee, J.H. Investigation of extreme environment conditions and design thermal gradients during construction for prestressed concrete bridge girders. *J. Bridge Eng.* **2011**, *17*, 547–556. [[CrossRef](#)]

Disclaimer/Publisher's Note: The statements, opinions and data contained in all publications are solely those of the individual author(s) and contributor(s) and not of MDPI and/or the editor(s). MDPI and/or the editor(s) disclaim responsibility for any injury to people or property resulting from any ideas, methods, instructions or products referred to in the content.